Noise Analysis on Wide-Band PLC with High Sampling Rate and Long Observation Time

Yuichi HIRAYAMA† Hiraku OKADA‡ Takaya YAMAZATO‡ Masaaki KATAYAMA‡

† Katayama Lab., Dept. of Info. Elec.,
Graduate School of Eng., Nagoya University.
Nagoya, 464-8603, Japan.
Phone: +81-52-789-2729, Fax: +81-52-789-3173
E-mail: yhiraya@katatyama.nuee,nagoya-u.ac.jp

‡ Center for Information Media Studies,
Nagoya University. Nagoya, 464-8603, Japan.
Phone: +81-52-789-2743, Fax: +81-52-789-3173
E-mail: {okada,yamazato,katayama}@nuee.nagoya-u.ac.jp

Abstract

This manuscript reports the results of the measurement of wide-band PLC noise with high speed (50MHz) sampling and long (10.4s) observation duration. The measured noise is divided in frequency, and stochastic properties of the noise waveforms in each frequency bands, such as autocorrelations, probability density functions, and correlation coefficients between noise waveforms of different frequency bands are discussed. Cyclostationary features of the noise in each band is confirmed. It is found that the amplitude distribution in each band is different, and that Gaussian noise model is not a good approximation in higher frequency bands.

1. Introduction

The noise on power-lines is mainly caused by electric appliances connected to the lines whose statistical behavior is quite different from that of stationary white Gaussian noise. It is known that the noise characteristic in power-line changes synchronous with a half cycle of the power supplying AC voltage [1, 2, 3]. For narrow-band PLC systems (e.g. from 10kHz to 450kHz), the cyclo-stationary Gaussian noise model to represent the noise has been proposed in [4, 5, 6]. With this model, the relation of the bit error rate in time-frequency domain has been analyzed, and also performance improvement schemes have been proposed in [7, 8].

In many countries, including Japan, high-speed PLC using wide-band frequency range up to about 30MHz has been drawing much attention as an alternative communication system. In order to realize reliable high-speed PLC, it is essential to understand the features of power-line noise. There is, however, few report on noise characteristics of wide-band PLC.

A part of this work is financially supported by TDK Co. and CHUBU Electric Power Co., Inc.

In this manuscript, we report the results of measurement of wide-band PLC noise with 50MHz sampling speed and observe during about 10.4 seconds. To examine the noise characteristic, the statistical properties such as autocorrelation, probability density function (PDF) and correlation coefficient are discussed.

2. Noise measurement system

The environment and the system of the noise measurement is shown in Fig.1. The system consists of a pick-up circuit, an A/D converter and a computer.

The pick-up circuit is shown in Fig.2. In the pick-up circuit, the AC component is attenuated by capacitors, common-mode noise component is removed by a high frequency transformer, and balance-to-unbalance transform of the circuit is performed by a balun. Then, the noise component is obtained at the terminal labeled “noise” in the figure. The AC voltage waveform which has about two volts of peak-to-peak voltages is taken at the terminals labeled “AC” after a step down transformer and voltage dividing resistors. This AC voltage waveform is used as a triggering signal to start a measurement. The circuit elements are shown in Tab.1.

The A/D converter digitizes the noise component to 8bits data with the rate of 50MHz over 10.4 seconds, which corresponds to 500 cycles of the power supplying AC voltage, and stores the samples in 512M byte memory. The measurement specifications are shown in Tab.2.

3. An example of the measured noise

3.1. Noise components in time domain

Using the measurement system, noise is measured in our laboratory. An example of the noise waveform is shown in Fig.3. This figure shows the noise over 0.05 seconds

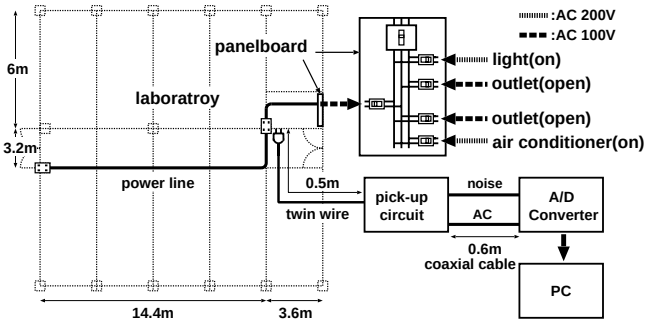

Figure 1: Measurement system.

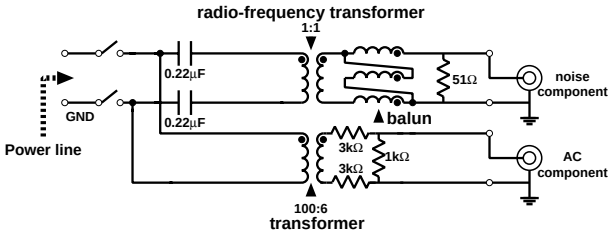

Figure 2: Pick-up circuit.

which corresponds to three AC voltage cycles. This figure shows that the noise characteristics change synchronous with a period $T_{AC}/2$, where T_{AC} is a cycle duration of the power supplying AC voltage. All the data analyzed in this manuscript, including this sample waveform, are taken at 22:00 on Nov. 25 2002.

3.2. Noise spectrum in frequency domain

By calculating Fourier transform for the measured noise, the noise spectrum up to the Nyquist frequency

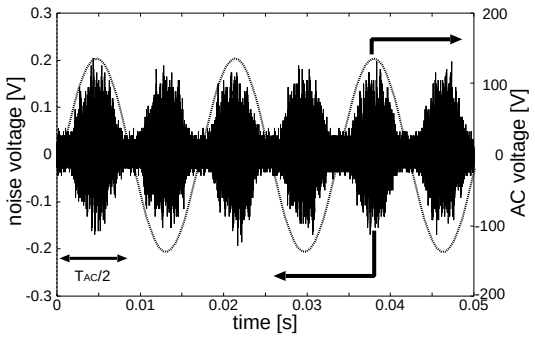

Figure 3: Measurement noise waveform.

Table 1: Circuit elements.

Circuit element	Maker Model No.	Specifications
AC transformer	TOYOZUMI HT-61	Turn ratio 100:6
RF transformer	- -	Turn ratio 1:1 Core : TDK HF70
Balun	- -	5 turns Core : TDK HF70
Metal-oxide film resistor	- -	51Ω, 1kΩ, 3kΩ
Polyester capacitor	- -	0.22μ F

Table 2: Measurement specifications.

Measurement instrument	Maker Model No. Serial No.	Specifications
A/D converter	ELMEC EC-6800 B2CH1E01	Range 1V Resolution 8bit S.P. rate 50Msps

25MHz is obtained, which is shown in Fig.4. From this figure, it can be observed that the noise spectrum is concentrated under 10MHz.

3.3. Noise amplitude distribution in time-frequency domain

By using a band-pass filter which is realized by digital signal processing on the computer, we calculate noise waveform in a given frequency subband. Then, repeating this process for other frequency subbands, noise amplitude distribution in time-frequency domain can be obtained. An example of noise distribution in time-frequency domain is shown in Fig.5, where the passband width of band-pass filter W is selected $W = 500$kHz. This figure shows the noise over 0.05 seconds which corresponds to $3T_{AC}$ and the noise up to 12MHz. From this figure, it can be seen that the noise waveform in each subband changes periodically and synchronous with the period $T_{AC}/2$. In the following section, the noise waveforms in the subbands 3MHz-3.5MHz and 9MHz-9.5MHz, which have distinctive features are considered. In addition, the noise waveform in the subband 0-2MHz is also considered to be used as the noise waveform outside of communication band discussed in section 5. The waveforms in these subbands are shown in Figs.6–8.

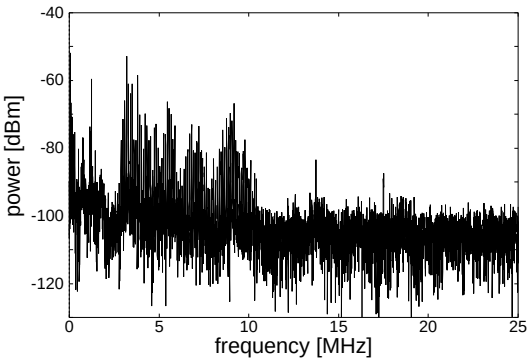

Figure 4: Noise spectrum for the measured noise.

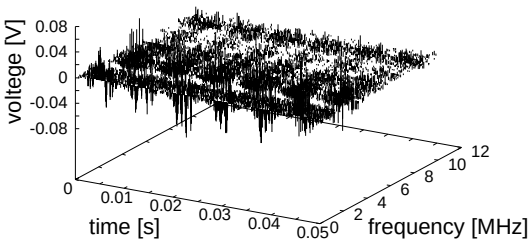

Figure 5: Noise amplitude distribution in time-frequency domain.

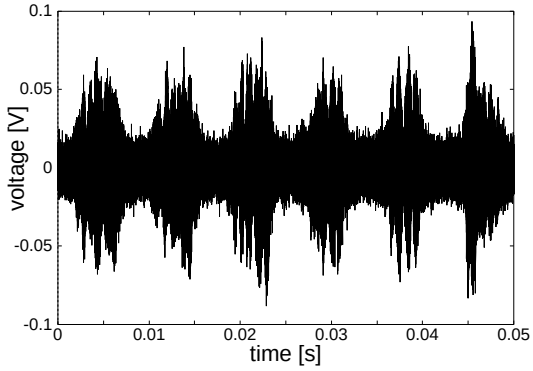

Figure 6: Noise waveform in 0-2MHz.

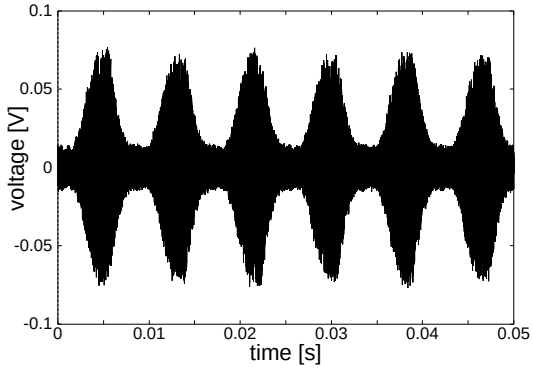

Figure 7: Noise waveform in 3MHz-3.5MHz.

4. Noise statistical characteristics

4.1. Autocorrelation

Let N be the number of samples of a given subband noise, then the autocorrelation function of the absolute value of noise is defined as

$$R_{nn}(\tau) = \frac{1}{\sigma_N^2 \cdot N} \sum_{i=0}^{N-1} \big|n[i]\big|\big|n[i+\tau]\big| \tag{1}$$

where $n[i]$ is a i-th sample of the noise waveform of the given subband, τ is a delay in samples and

$$\sigma_N^2 = \frac{1}{N} \sum_{i=0}^{N-1} \big|n[i]\big|^2. \tag{2}$$

The results are shown in Figs.9–11. From these figures, it is seen that noise of each subband has wide sense cyclo-stationary features with the period $T_{AC}/2$.

4.2. The distribution of noise amplitude

Since the noise waveform in each subband is discrete in time and amplitude, the normalized amplitude distribution of the waveform can be defined as

$$p(x) = \frac{1}{N} \sum_{i=0}^{N-1} \Theta\left(\left\lfloor \frac{x}{\Delta\sqrt{\sigma_N^2}} \right\rfloor < \frac{n[i]}{\Delta} \le \left\lfloor \frac{x}{\Delta\sqrt{\sigma_N^2}} \right\rfloor + 1 \right) \tag{3}$$

where $\Theta(\ )$ is the function which takes 1 if the condition in its parentheses is satisfied, otherwise takes value zero. The notation $\lfloor x/\Delta\sqrt{\sigma_N^2} \rfloor$ is the largest integer smaller than $x/\Delta\sqrt{\sigma_N^2}$ and Δ is the range of amplitude.

As described in 4.1, the noise waveform in each band is cyclo-stationary in wide sense. Thus let us define cyclic distribution of the subband noise at a given phase of AC voltage, $t = m\delta + T_{AC}/2$, where $1/\delta$ is the sampling rate, as

$$p_m(x) = \frac{1}{M} \sum_{i=0}^{M-1} \Theta\left(\left\lfloor \frac{x}{\Delta\sqrt{\sigma_M^2}} \right\rfloor < \frac{n\left[m + i\frac{T_{AC}}{2\delta}\right]}{\Delta} \le \left\lfloor \frac{x}{\Delta\sqrt{\sigma_M^2}} \right\rfloor + 1 \right) \tag{4}$$

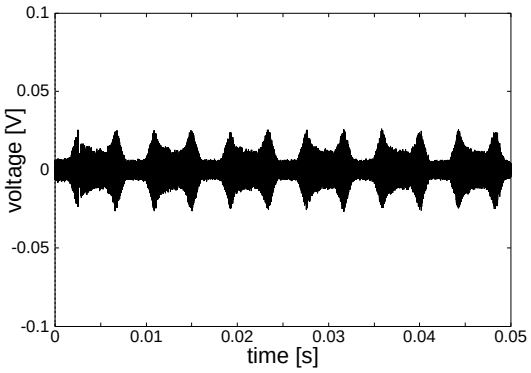

Figure 8: Noise waveform in 9-9.5MHz.

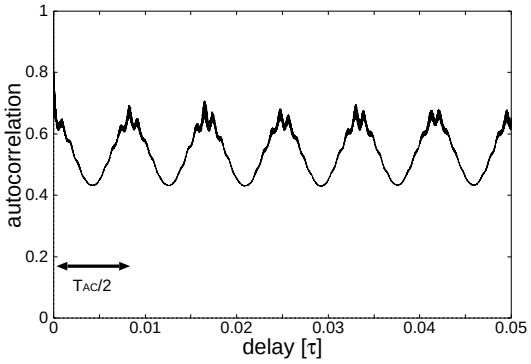

Figure 9: Autocorrelation for noise in 0-2MHz.

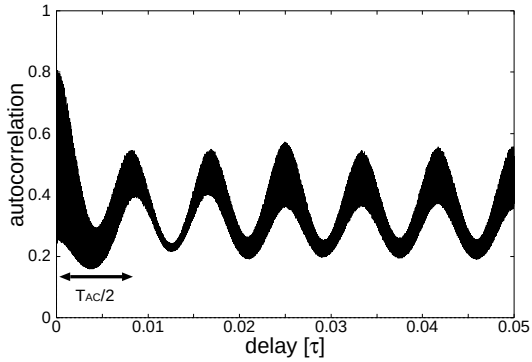

Figure 10: Autocorrelation for noise in 3MHz-3.5MHz.

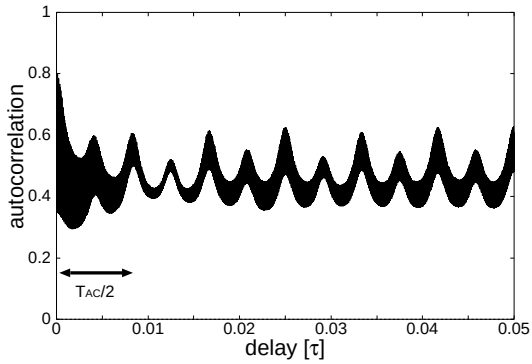

Figure 11: Autocorrelation for noise in 9-9.5MHz.

where M is the number of samples corresponding to every $T_{AC}/2$ and

$$\sigma_M^2 = \frac{1}{M} \sum_{i=0}^{M-1} \left| n[m + i(T_{AC}/2\delta)] \right|^2. \quad (5)$$

Figs.12–14 show the PDF by Eq.(3) and Eq.(4) for each subband with $\Delta = 2/256$[V], where cyclic PDF is taken at the peak of AC voltage and at the time where AC voltage crosses zero. The figures also show Gaussian distribution with the same variance. From these figures, it can be seen that the amplitude distribution in each frequency band is different. In the subband 0-2MHz, the distribution is approximate to Gaussian, while in the subband 3MHz-3.5MHz and 9-9.5MHz, the distributions tend to show the features of impulsive noise. Furthermore, in each frequency subband, their cyclic distributions may have the same shape regardless of phase of AC voltage.

5. Normalized correlation coefficient

Because the noise level changes synchronous with $T_{AC}/2$ in each frequency band, the noise waveforms of different frequency bands are dependent to each other.

To examine the dependence between $n_r[i]$ and $n_s[i]$, we evaluate their correlation coefficient. Suppose that $n_r[i]$ and $n_s[i]$ have a frequency content concentrated in a narrow band of frequencies in the vicinity of a frequency f_{cr} and f_{cs}. Here, instead of using $n_r[i]$ and $n_s[i]$ to evaluate the correlation, we use the equivalent low-pass noise, defined as

$$n_{rl}[i] = n_{r+}[i] e^{-j2\pi f_{cr} i\delta} \quad (6)$$

$$n_{sl}[i] = n_{s+}[i] e^{-j2\pi f_{cs} i\delta} \quad (7)$$

where $n_{r+}[i]$ and $n_{s+}[i]$ are band-pass components of $n_r[i]$ and $n_s[i]$. Then the instantaneous noise power at the i-th sample timing is defined $p_{rl}[i] = |n_{rl}[i]|^2$. Assuming cyclo-stationarity of outband noise with the period $T_{AC}/2$ and ergodicity at every $T_{AC}/2$, the cyclic average power at

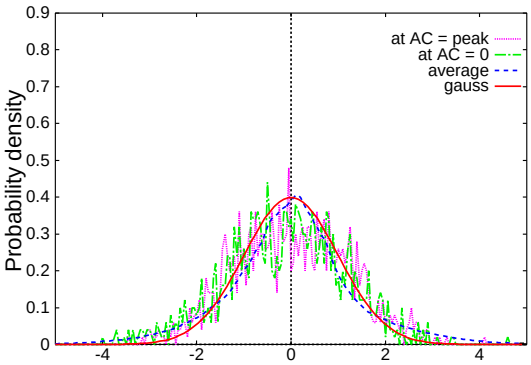

Figure 12: Amplitude distribution in 0-2MHz.

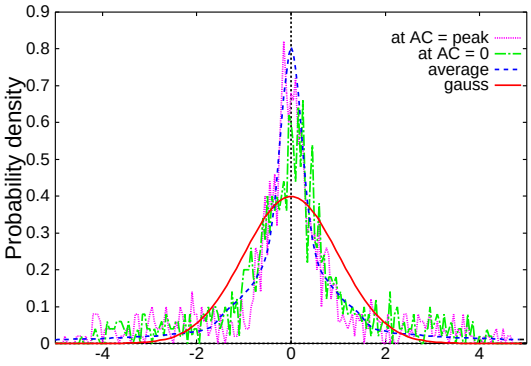

Figure 13: Amplitude distribution in 3MHz-3.5MHz.

$t = m\delta + T_{AC}/2$ $P_{rl}[m]$ is

$$P_{rl}[m] = E\left[p_{rl}[m]\right] = \frac{1}{M}\sum_{i=0}^{M-1} p_{rl}\left(m + i\frac{T_{AC}}{2\delta}\right). \quad (8)$$

Similarly, we define the i-th noise power in communication frequency band $p_{sl}[i]$, and the m-th average power $P_{sl}[m]$.

First, we discuss about the noise scattering diagram between $p_{rl}[m] - P_{rl}[m]$ and $p_{sl}[m] - P_{sl}[m]$. The scattering diagram between 0-2MHz and 3MHz-3.5MHz and between 0-2MHz and 9MHz-9.5MHz are shown in Figs.15,16. From these figures, it can be seen that when $p_{rl}[m] - P_{rl}[m]$ is small, $p_{sl}[m] - P_{sl}[m]$ also tends to be small; however when the instantaneous noise power is large, there is not clear relationship between two noise component.

Next, let us discuss the normalized correlation coefficient between $p_{rl}[m] - P_{rl}[m]$ and $p_{sl}[m] - P_{sl}[m]$, which is expressed as

$$\rho_{rs}[m] = \frac{1}{M}\sum_{i=0}^{M-1}\left(p_{rl}\left[m+i\frac{T_{AC}}{2\delta}\right]-P_{rl}[m]\right)\left(p_{sl}\left[m+i\frac{T_{AC}}{2\delta}\right]-P_{sl}[m]\right)$$

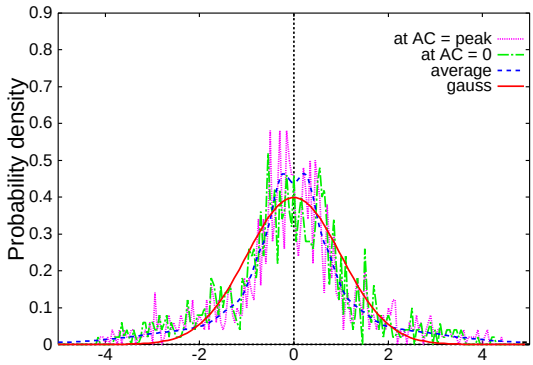

Figure 14: Amplitude distribution in 9MHz-9.5MHz.

$$\times \frac{1}{\sqrt{\left(\frac{1}{M}\sum_{i=0}^{M-1}\left|p_{rl}[m+i\frac{T_{AC}}{2\delta}]\right|^2 - (P_{rl}[m])^2\right)}}$$

$$\times \frac{1}{\sqrt{\left(\frac{1}{M}\sum_{i=0}^{M-1}\left|p_{sl}[m+i\frac{T_{AC}}{2\delta}]\right|^2 - (P_{sl}[m])^2\right)}}$$

$$\left(0 \le m < \frac{T_{AC}}{2\delta}\right). \quad (9)$$

The probability density and cumulative density distribution of normalized correlation coefficient is shown in Fig.17. From Fig.15–17, it can be seen that except the case both $p_{rl}[m] - P_{rl}[m]$ and $p_{sl}[m] - P_{sl}[m]$ are small, they are independent to each other.

6. Conclusion

In this manuscript, we report the results of measurement of wide-band PLC noise with 50MHz sampling speed and observe during about 10.4 seconds. Using the measured noise, the noise properties are analyzed. Then, following three stochastic characteristics can be seen. First, the noise characteristics in each subband change synchronous with $T_{AC}/2$. Second, the amplitude distributions in each subband is different, in the lower subbands, noise is approximate to Gaussian but in higher subband, noise tends to be impulsive. In both case, cyclic distributions have the same shape regardless of phase of AC voltage. Finally, instantaneous noise power in each subband is dependent when these power are smaller than that of averages.

References

[1] Y. Hirayama, H. Okada, T. YAMAZATO, and M. KATAYAMA, “Statistical Noise Characterization for Wide Band Power Line Communication System”, IEICE SST2002-13, Jul. 2002.

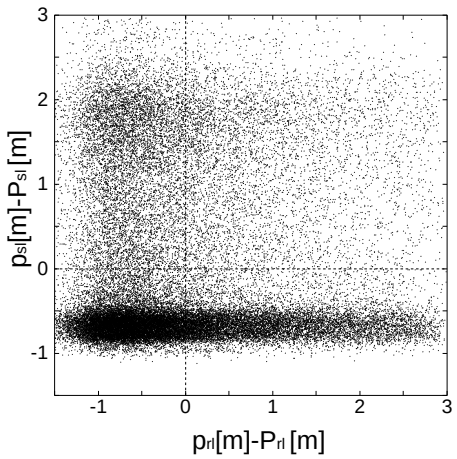

Figure 15: Scattering diagram between noise in 0-2MHz and noise in 3MHz-3.5MHz.

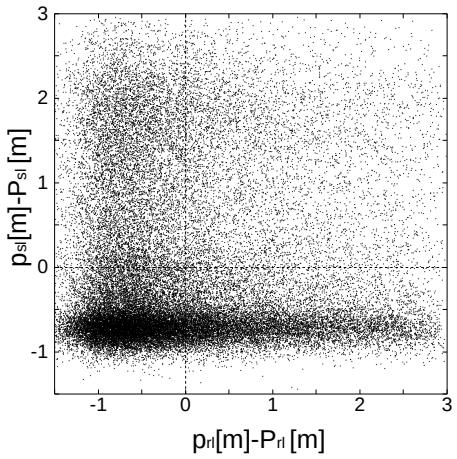

Figure 16: Scattering diagram between noise in 0-2MHz and noise in 9MHz-9.5MHz.

[2] M. Katayama, “Technical Challenges for the Realization of Robust Reliable and High-Speed Power-Line Communication Systems”, IEICE SST2000-60, Dec. 2000.

[3] Manfred Zimmermann and Klaaus Dostert, “An Analysis of the Broadband Noise Scenario in Powerline Networks”, ISPLC2000, pp.131–138, Ireland, Apl. 2000.

[4] H. Niwa, O. Ohno, M. Katayama, T. Yamazato, and A. Ogawa, “A Spread spectrum system with dual processing gains designed for cyclic noise in power line communications”, IEICE Trans. Fundamentals, Vol.E80-A, No.12, pp.2526-2533, Dec. 1997.

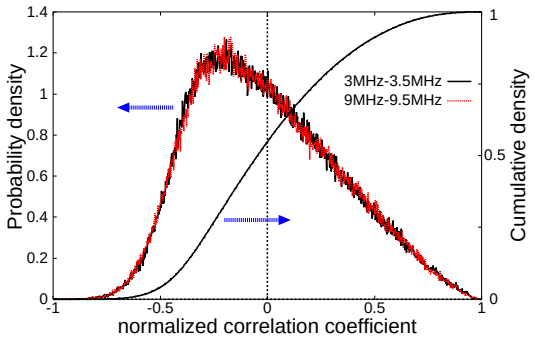

Figure 17: The distribution of normalized correlation coefficient.

[5] O. Ohno, M. Katayama, T. Yamazato, and A. Ogawa, “A Modeling of the Noise for Power Line Communication Systems”, IEICE technical report,DSP97-61, SST97-21,CS97-46, pp.7-12, Jul. 1997.

[6] M. Katayama, S. Itou, T. Yamazato, A. Ogawa, “Modeling of Cyclostationary and Frequency Dependent Power-Line Channels for Communications” ISPLC2000, pp.123–127, Ireland, Apl. 2000.

[7] M. Katayama, “Introduction to Robust, Reliable, and High-Speed Power-Line Communication Systems”, IEICE Trans. Fundamentals, vol.E84-A, no.12 Dec.2001.

[8] K. Sugimto, H. Okada, T. Yamazato, and M. Katayama, “Performance Improvement of OFDM System with Consideration on the Characteristics of Power-Line Noise”, IEICE Trans. Fundamentals, vol.E85-A, no.12, pp.2822-2829, Dec.2002.